PCCP

Accepted Manuscript

This is an *Accepted Manuscript*, which has been through the Royal Society of Chemistry peer review process and has been accepted for publication.

Accepted Manuscripts are published online shortly after acceptance, before technical editing, formatting and proof reading. Using this free service, authors can make their results available to the community, in citable form, before we publish the edited article. We will replace this *Accepted Manuscript* with the edited and formatted *Advance Article* as soon as it is available.

You can find more information about *Accepted Manuscripts* in the Information for Authors.

Please note that technical editing may introduce minor changes to the text and/or graphics, which may alter content. The journal's standard Terms & Conditions and the Ethical guidelines still apply. In no event shall the Royal Society of Chemistry be held responsible for any errors or omissions in this *Accepted Manuscript* or any consequences arising from the use of any information it contains.

ROYAL SOCIETY OF CHEMISTRY

www.rsc.org/pccp

Nanogap Effects on Near- and Far-Field Plasmonic Behaviors of Metallic Nanoparticle Dimers†

Yu Huang,[a] Qin Zhou,[b] Mengjing Hou,[a] Lingwei Ma[a] and Zhengjun Zhang*[c]

[a] *State Key Laboratory of New Ceramics and Fine Processing, School of Materials Science and Engineering, Tsinghua University, Beijing 100084, P. R. China*

[b] *Institute of Nuclear and New Energy Technolog, Tsinghua University, Beijing 100084, P. R. China*

[c] *Key Laboratory of Advanced Materials (MOE), School of Materials Science and Engineering, Tsinghua University, Beijing 100084, P. R. China. E-mail: zjzhang@tsinghua.edu.cn*

† Electronic Supplementary Information (ESI) available: Details on near-field $\overline{EF}$ and corresponding far-field extinction cross section C_{ext} spectra of realted dimer structures, and movies of three dimensional surface charge distributions. See DOI: 10.1039/

Physical Chemistry Chemical Physics Accepted Manuscript

Graphical abstract

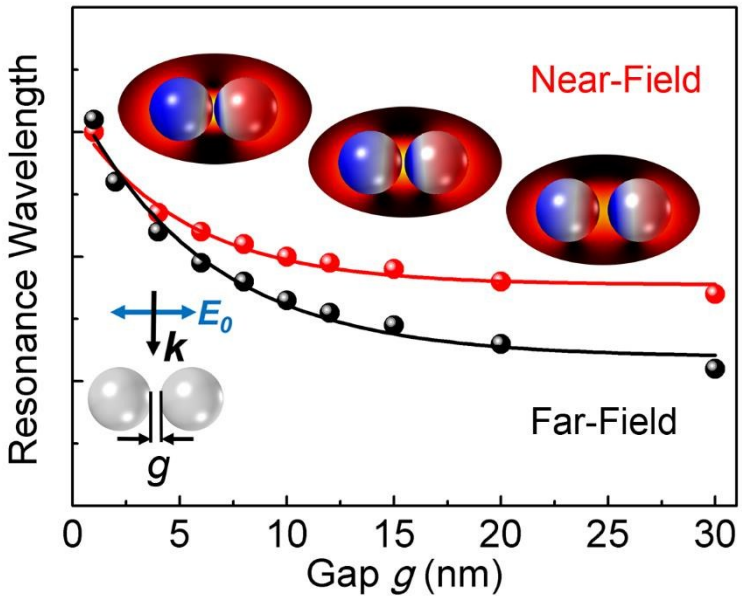

The near-field resonance shift of metallic nanosphere dimers decays nearly exponentially as the gap size increases, with a lower decay length than the far-field resonance shift.

Abstract

In the field of plasmonics, the nanogap effect is often related to one aspect like the near-field enhancement at a single excitation wavelength or the far-field resonance shift. In this study, taking full advantages of finite element method (FEM) calculations, we present a comprehensive and quantitative analysis of the nanogap effect on plasmonic behaviors of metallic nanoparticle dimers. Firstly, a near-field spectroscopy is proposed in order to extract the near-field resonance wavelengths. Focusing on the bonding dipole mode, it is found that the near-field enhancement factors exhibit a weak power-law dependence on the gap size, while the near-field resonance shift decays nearly exponentially as the gap size increases, with a lower decay length than that for the

Physical Chemistry Chemical Physics Accepted Manuscript

far-field resonance shift. The spectral deviation between these two shifts is suggested to be taken into account for spectroscopy applications of plasmonic devices, although it may be negligible for dimer structures with rather small gaps.

Introduction

Metallic nanoparticles, usually of Ag or Au, can undergo light-driven collective oscillations of the conduction electrons known as localized surface plasmon resonances (LSPRs). By virtue of being small, such particles are able to guide and concentrate light at the sub-wavelength scale[1] and provide extremely large localized enhancements of local electric fields.[2] These unique properties benefit applications of metallic nanoparticles in varied fields such as plasmonic waveguiding,[3] chemical and biological sensing,[4-7] as well as surface-enhanced spectroscopies.[8-15] The spectral responses and spatial field distributions of LSPRs are greatly determined by the particle size, shape, surface morphology and dielectric environment.[16-18] For the purpose of fundamental studies and spectroscopy applications, the geometry of nanoparticle dimers has attracted much attention due to the dramatic electromagnetic (EM) field confinement and enhancement in the nanogap, i.e., the so-called "hot spots".[12, 19, 20]

Commonly, the enhanced fields around a single particle are much weaker than that in the nanogap of a dimer, unless the single particle has a very sharp feature.[17, 21, 22] When two individual metallic nanoparticles are brought into close proximity to each other, the nanogap effect occurs as their surface plasmons couple electromagnetically in the non-radiative near-field region, which leads to many interesting modifications of their plasmonic behaviors besides the generation of hot spots, such as the evolution of hybridized plasmon modes, the shift of plasmon resonances and so

Physical Chemistry Chemical Physics Accepted Manuscript

on.[20, 23-27] It is found that the local electric field in the gap can be more enhanced when decreasing the gap size until reaching the quantum tunneling region.[28, 29] This enhancement even allows surface-enhanced Raman scattering (SERS) signal to be detected with single-molecule sensitivity.[30, 31] On the other hand, the far-field resonance wavelength shift of nanoparticle dimers has been studied both experimentally and theoretically. The shift for polarization along the interparticle axis decays nearly exponentially with the gap size,[32-34] which could substantially benefit to improve the sensitivity of localized surface plasmon sensing when applied to very local changes of the refraction index as induced by the presence of few or even single molecules.[4, 7]

The far-field spectroscopy has also been typically applied for the optimization of plasmonic devices with enhanced near-field properties. A major goal is to achieve the highest local EM field enhancement. However, it was only recently fully appreciated that there exists a distinct deviation of spectral positions between the near- and far-field plasmon resonances,[35-39] while it remains challenging to collect the entire near-field spectral and spatial characteristics and in many cases only single frequencies are considered.[40-42] In addition, limited by current nanofabrication technique, the interparticle gap sizes on the order of sub-10 nanometers with good reproducibility and uniformity remain difficult to control,[13, 43, 44] resulting in uncertainties of the promoted nanogap effect.

In this study, we present a comprehensive analysis of the nanogap effect on plasmonic properties of metallic nanoparticle dimers *via* full electrodynamic calculations. To extract the near-field resonance wavelengths and acquire local electric field enhancement factors (EFs), a near-field spectroscopy is proposed. Focusing on the bonding dipole mode,[28, 45] these near-field properties induced by the nanogap effect together with the far-field ones are investigated and summarized quantitatively.

Physical Chemistry Chemical Physics Accepted Manuscript

Theory and computational method

Finite element method (FEM)[46, 47] in COMSOL Multiphysics software package[48] (installed on a Quad Intel Xeon CPU, 64 GB RAM workstation) was used for our three dimensional electrodynamic calculations. Using adaptive meshing, the highest spatial resolution of the grid is ~0.33 nm. The dielectric functions $\varepsilon(w)$ of Ag and Au were modeled by a Lorentz-Drude dispersion model[49] based on the experimental data in Palik's book.[50]

$$\varepsilon(w) = 1 - \frac{f_0 {w_p}^2}{w(w - i\Gamma_0)} + \sum_{j=1}^{m} \frac{f_j {w_p}^2}{({w_j}^2 - w^2) + iw\Gamma_j} \quad (1)$$

where w_p is the plasma frequency with oscillator strength f_0 and damping constant Γ_0 that are applied in the well-known Drude model, while the last term in equation (1) is the result of Lorentz modification, m is the number of oscillators with frequency w_j ,strength f_j and damping constant Γ_j. The values of above parameters can be found in the reference.[49]

For far-field properties, extinction spectra were calculated by integrating the time-averaged extinction Poynting vectors $\boldsymbol{S}_{ext}$ (i.e. EM power flow) over an auxiliary surface Ω enclosing the nanoparticle dimers [51, 52]

$$\boldsymbol{S}_{ext} = \frac{1}{2}\mathrm{Re}\{\boldsymbol{E}_{inc} \times \boldsymbol{H}_{sca}{}^{*} + \boldsymbol{E}_{sca} \times \boldsymbol{H}_{inc}{}^{*}\} \quad (2)$$

$$C_{ext} = \frac{-\iint \boldsymbol{S}_{ext} d\Omega}{|\mathbf{W}_{inc}|} \quad (3)$$

Physical Chemistry Chemical Physics Accepted Manuscript

where $\boldsymbol{E}_{\mathrm{inc}}$, $\boldsymbol{E}_{\mathrm{sca}}$, $\boldsymbol{H}_{\mathrm{inc}}$ and $\boldsymbol{H}_{\mathrm{sca}}$ are the incident and scattered electric and magnetic field respectively, C_{ext} is the extinction cross section, $|\mathbf{W}_{inc}| = {}^{1}/_{2}\, c\varepsilon_0 \mathrm{E}_0{}^{2}$ is the power flow per unit area of the incident plane wave, E_0 (set at 1 V/m for convenience) is the modulus of $\boldsymbol{E}_{\mathrm{inc}}$, c is the velocity of light and ε_0 is the permittivity of vacuum; While the near-field spectroscopy is represented by the averaged local electric field EF versus the excitation wavelength, in the expression of

$$\overline{EF} = \frac{\iiint (|\boldsymbol{E}|^4/|\boldsymbol{E}_{inc}|^4) dV}{V} \quad (4)$$

where V is the volume within a certain distance above the metal surface (here we take 2 nm, see Fig. S1(a), ESI†) and $\boldsymbol{E}$ is the local electric field. The physical significance of $\overline{EF}$ can be understood as the averaged EF of SERS based on its EM theory,[47, 53] on the assumption that Raman probe molecules are arranged randomly and uniformly on the surface of metallic nanoparticles. Instead of a surface integral, the volume integral was performed with consideration of numerical instabilities at the metal surface and the dimensions of adsorbed molecules.[54]

Results and discussion

Fig. 1 shows the calculated near-field $\overline{EF}$ and the far-field extinction spectra with 5 nm wavelength spacing for Ag nanosphere (radius r = 60 nm) dimers. The gap size g varies from 1 to 30 nm. This gap size range ensures the relatively strong near-field coupling of the surface plasmons, because the evanescent waves do not propagate away from the metal surface and their EM energies decrease exponentially as the distance from the surface increases.[26, 37] The minimum gap size is fixed to be 1 nm in order to avoid the invalidation of classic electrodynamics for the reason that

Physical Chemistry Chemical Physics Accepted Manuscript

below 1 nm the quantum and non-local effects need to be considered.[25, 28, 29] The incident polarization in the calculation keeps along the interparticle axis. The computational time for an entire spectrum (i.e. 100 spectral points in the wavelength range of 300-800 nm) is ~24 h.

As is shown in Fig. 1(a), the $\overline{EF}$ intensity appears rather sensitive to the gap size change. It decreases sharply over a large wavelength range as the gap size increases. The intensity level for g = 1 nm is as high as 10^7, while it is even lower than 10^3 for g = 30 nm. On the other hand, multiple resonance peaks arise in the $\overline{EF}$ spectra, especially for dimers with narrower gaps. Correspondingly there are a series of peaks in the extinction spectra (Fig. 1(b)). Among these peaks, the ones indicated by up triangle symbols are mapped to be the same kind of plasmon resonance namely the bonding dipole mode, which we will prove in Fig. 2. Both the near- and far-field resonances are blueshifted as the gap size increases. The reason that we focus on the bonding dipole mode is that it is a fundamental mode for the dimer system. Owning to stronger coupling to incident light the bonding dipole mode exhibits a higher extinction cross section and a broader resonance than those multipole coupling modes generated in shorter wavelength regions, as seen from Fig. 1(b). Note that the near field enhancement is almost 'flat' in the visible range, it is a result of the continuous arising of bonding dipole resonances in longer wavelength regions and bonding multipole resonances in shorter wavelength regions (see Fig. S2, ESI†). As is known, for large individual plasmonic nanospheres (e.g. r > 50 nm), multipole resonances can be excited besides the fundamental dipole resonance.

Typical local electric field distributions at the near-field bonding dipole resonance wavelengths are shown in the upper row of Fig. 2, in the form of logarithmic $|E/E_0|^4$ (i.e. EF). Fig. 2(a)-(d) correspond to g = 1, 2, 8, 30 nm from left to right. The local field enhancement in the gap are extremely large for g = 1 nm, reaching up to an order of 10^{10} in terms of $|E/E_0|^4$; however, it

Physical Chemistry Chemical Physics Accepted Manuscript

decreases to just an order of 10^4 as the gap size increases to 30 nm. It is also found that the value of the defined $\overline{EF}$ can be 3 orders of magnitude lower than the maximum EF (EF_{max}). In the bottom row, the corresponding three dimensional surface charge distributions are plotted. Red color represents positive charge while blue is negative. The mapping indicates clearly the bonding dipole mode. The induced surface charge density ρ are calculated directly by applying classical Gauss's law in its differential form during FEM calculations, since metals of Ag and Au are good electrical conductor and hence almost all the induced charge distributes on the metal surface:

$$\frac{\rho}{\varepsilon_0} = \nabla \cdot \boldsymbol{E} = \boldsymbol{n} \cdot \boldsymbol{E} \quad (5)$$

where ε_0 is the permittivity of vacuum and $\boldsymbol{n}$ is the outward normal vector of the metal surface. It is worth mentioning that the plotted surface charge distributions are with the maximum transient surface charge polarizations within one full oscillation (see Movie S1 in ESI†). They highlights the strong correlation between the surface plasmon geometry and the local electric field distributions. For strong bonding dipole coupling like in the case of g = 1 nm (Fig. 2(e)), the single dipole are deformed badly. Thus by applying above near-field plasmon mapping method, it is easy for us to determine the plasmon mode through its pole geometries, and it may be feasible to judge the coupling strength through the deformation of each single pole geometry that participates in the coupling process.

For further analysis of the nanogap effect, the entire near-field $\overline{EF}$ and the far-field extinction spectra of of Ag nanosphere (r = 30 nm) and Au nanosphere (r = 30 and 60 nm) dimers with 1 to 30 nm gap are calculated (see Fig. S3-S6, ESI†). Both the values of $\overline{EF}$ and EF_{max} of the near-field bonding dipole mode are extracted and then plotted in Fig. 3 as a function the gap size g. Interestingly, it turns out to be a nearly linear relation in all the log-log plots. The slopes n are

Physical Chemistry Chemical Physics Accepted Manuscript

about -3.0 and -4.5 for log($\overline{EF}$) and log(EF_{max}) against log(g) respectively. These plots suggest a weak but maybe general power-law dependence of the local electric field E on the gap size g:

$$\overline{EF}(and\ EF_{\max}) = 10^{A} \cdot g^{n} \quad (6)$$

In recent research works similar relationship has been given theoretically and experimentally, despite the fact that their excitation wavelengths are fixed. An $|E|^4 \sim 1/g^4$ behavior can be acquired from the predictions of antenna theory yet it concerns with metallic structures that are perfect electrically conducting (PEC) metals, while it is argued that the behavior is more closer to $|E|^4 \sim 1/g^2$ for actual plasmonic structures.[25, 55, 56] There are experimental measurements of SERS EF showing $|E|^4 \sim 1/g^{2.3}$ and $1/g^{1.5}$ dependence, also measurements of surface enhanced infrared absorption supporting $|E|^2 \sim 1/g^{1.0}$ dependence. The complemented simulations for above measurements are in favor of a relatively higher exponents n which are $|E|^4 \sim 1/g^{2.8}$ and $|E|^2 \sim 1/g^{1.5}$ respectively.[13, 23, 57] Whether it is excited by a fixed wavelength or the changing resonance wavelengths can make a difference in n value (see Fig. S7, ESI†). And it is certain that different expressions of EFs contributes to the deviation of n value. To confirm n and arrive at some universal conclusion, further investigations are desired.

In Fig. 4, we summarize the calculated resonance wavelengths for different dimer structures above. As the gap size g increases monotonically, the near-field coupling becomes weaker while both the near- and far-field resonances are blueshifted with a lower speed. In addition, the shift speed of the near-field resonance is apparently lower than that of the far-field resonance for three out of the four dimer structures, resulting in greater and greater deviations between the near- and far-field resonances as g increases. The deviation is about 60 nm at g = 30 nm for Ag dimers of r = 60 nm nanospheres. Yet, for the Ag dimer of r = 30 nm nanospheres, the deviation is rather small.

Physical Chemistry Chemical Physics Accepted Manuscript

In order to explain the deviation, both the near-field $\overline{EF}$ and the far-field extinction spectra for the isolated nanospheres are calculated, as seen in Fig. 5. In principle, for a nanosphere dimer, as the gap size increases endlessly and approaches infinity, it can be treated as an isolated nanosphere. Both its near- and far-field resonance wavelengths will tend towards that of the isolated nanosphere. Actually the near- and far-field resonances of the corresponding isolated nanosphere in our calculations do peak at the shorter wavelength regions, while the near-field resonance is further found to be redshift against the far-field one. In particular the deviation between its near- and far-field resonance is only 5 nm for the isolated Ag nanosphere with r = 30 nm. This is also in agreement with what is reported in recent works and the deviation is found to be largely affected by the size, shape and material (in terms of the plasmon damping) of the particles. [36-41, 58] Although the spectral coincidence was often implicitly assumed in the past, the deviation between near- and far-field resonances should be considered for applications and optimizations of plasmonic devices, especially for large particles, since we have gained a better understanding of it now.

Another interesting finding is that the near- and far-field resonance deviation can be indeed negligible for dimers with rather small gaps like g =1 or 2 nm despite the fact that they are both extremely redshift relative to that of the isolated nanosphere. Taking SERS for example, such dimers are treated as typical hot spot systems. The spectral deviation between near- and far-field resonances (within 10 nm) is much smaller than the Stokes shift which is neglected sometimes in reality.[59]

The smooth curves in Figure 4 represent least-squares fits to single-exponential decay function

$$\lambda = \mathrm{a} \cdot e^{-l/g} + \lambda_0 \qquad (7)$$

Physical Chemistry Chemical Physics Accepted Manuscript

where λ is the resonance wavelength. The fitting parameters a, l and λ_0 are listed in Table 1. From Table 1, we see the value of l is a little lower for near-field resonances than that for the far-field ones. It scales with the shift speed as g increases. The fitting here is encouraged by the plasmon ruler equation summarized from the far-field resonance.[33, 34] It turns out to be suitable for the near-field resonance as well. The shift of the near- and far-field resonances and the deviation between them are closely related to the decay length l which is several nanometers for dimer structures discussed above. Based on a quasistatic dipole coupling model,[33] an intuitive picture of the distance decay of the plasmon coupling in metal nanostructures can be presented. Basically the dipole near-field of a plasmonic particle decays as the cube of the inverse distance. As a result, the plasmon coupling strength in the dimers becomes a function of g^{-3}, a dependence which can be approximated very nearly to an exponential decay.

Conclusion

Taking full advantages of FEM calculations, we have investigated quantitatively the near- and far-field plasmonic behaviors of metallic nanoparticle dimers and gained a comprehensive understanding of the nanogap effect. For the bonding dipole mode in the nanosphere dimers, both the averaged and maximum EM EFs exhibit a weak power-law dependence on the gap size, while the near-field resonance shift decays nearly exponentially as the gap size increases, with a lower decay length than that for the far-field resonance shift. The spectral deviation between these two shifts is suggested to be considered for spectroscopy applications of plasmonic devices such as SERS substrates, although it may be negligible for dimer structures with rather small gaps.

Physical Chemistry Chemical Physics Accepted Manuscript

Acknowledgements

The authors thank Professor W.S. Lai for the access to COMSOL Multiphysics software. This work was supported by the National Basic Research Program of China (973 program, grant No. 2013CB934301), the National Natural Science Foundation of China (Grant No. 51228101, 51301095), the Research Project of Chinese Ministry of Education (grant No. 113007A), and the Tsinghua University Initiative Scientific Research Program.

Physical Chemistry Chemical Physics Accepted Manuscript

References

1 D. K. Gramotnev and S. I. Bozhevolnyi, *Nat. Photonics*, 2014, 8, 13-22.

2 E. Hao and G. C. Schatz, *J. Chem. Phys.*, 2004, 120, 357-366.

3 S. I. Bozhevolnyi, V. S. Volkov, E. Devaux, J. Y. Laluet and T. W. Ebbesen, *Nature*, 2006, 440, 508-511.

4 P. K. Jain and M. A. El-Sayed, *Nano Lett.*, 2008, 8, 4347-4352.

5 S. Lal, S. E. Clare and N. J. Halas, *Acc. Chem. Res.*, 2008, 41, 1842-1851.

6 J. N. Anker, W. P. Hall, O. Lyandres, N. C. Shah, J. Zhao and R. P. Van Duyne, *Nat. Mater.*, 2008, 7, 442-453.

7 S. S. Acimovic, M. P. Kreuzer, M. U. Gonzalez and R. Quidant, *ACS Nano*, 2009, 3, 1231-1237.

8 J. F. Li, Y. F. Huang, Y. Ding, Z. L. Yang, S. B. Li, X. S. Zhou, F. R. Fan, W. Zhang, Z. Y. Zhou, D. Y. Wu, B. Ren, Z. L. Wang and Z. Q. Tian, *Nature*, 2010, 464, 392-395.

9 B. Sharma, R. R. Frontiera, A.-I. Henry, E. Ringe and R. P. Van Duyne, *Mater. Today*, 2012, 15, 16-25.

10 D. Brouard, M. L. Viger, A. G. Bracamonte and D. Boudreau, *ACS Nano*, 2011, 5, 1888-1896.

11 S. Lal, N. K. Grady, J. Kundu, C. S. Levin, J. B. Lassiter and N. J. Halas, *Chem. Soc. Rev.*, 2008, 37, 898-911.

12 W. Li, P. H. C. Camargo, X. Lu and Y. Xia, *Nano Lett.*, 2009, 9, 485-490.

13 C. Huck, F. Neubrech, J. Vogt, A. Toma, D. Gerbert, J. Katzmann, T. Haertling and A. Pucci, *ACS Nano*, 2014, 8, 4908-4914.

Physical Chemistry Chemical Physics Accepted Manuscript

14 E. Ringe, B. Sharma, A. I. Henry, L. D. Marks and R. P. Van Duyne, *Phys. Chem. Chem. Phys.*, 2013, 15, 4110-4129.

15 L. Ma, Y. Huang, M. Hou, Z. Xie and Z. Zhang, *Sci. Rep.*, 2015, 5.

16 F. J. GarciaVidal and J. B. Pendry, *Phys. Rev. Lett.*, 1996, 77, 1163-1166.

17 K. L. Kelly, E. Coronado, L. L. Zhao and G. C. Schatz, *J. Phys. Chem. B*, 2003, 107, 668-677.

18 E. Ringe, J. M. McMahon, K. Sohn, C. Cobley, Y. Xia, J. Huang, G. C. Schatz, L. D. Marks and R. P. Van Duyne, *J. Phys. Chem. C*, 2010, 114, 12511-12516.

19 H. X. Xu, E. J. Bjerneld, M. Kall and L. Borjesson, *Phys. Rev. Lett.*, 1999, 83, 4357-4360.

20 P. Nordlander, C. Oubre, E. Prodan, K. Li and M. I. Stockman, *Nano Lett.*, 2004, 4, 899-903.

21 E. Bailo and V. Deckert, *Chem. Soc. Rev.*, 2008, 37, 921-930.

22 A. Wiener, A. I. Fernandez-Dominguez, A. P. Horsfield, J. B. Pendry and S. A. Maier, *Nano Lett.*, 2012, 12, 3308-3314.

23 N. A. Hatab, C. H. Hsueh, A. L. Gaddis, S. T. Retterer, J. H. Li, G. Eres, Z. Y. Zhang and B. H. Gu, *Nano Lett.*, 2010, 10, 4952-4955.

24 Y. Yokota, K. Ueno and H. Misawa, *Chem. Commun.*, 2011, 47, 3505-3507.

25 J. M. McMahon, S. Li, L. K. Ausman and G. C. Schatz, *J. Phys. Chem. C*, 2012, 116, 1627-1637.

26 L. Tong, H. Xu and M. Kall, *MRS Bull.*, 2014, 39, 163-168.

27 J. S. Ahn, T. Kang, D. K. Singh, Y.-M. Bahk, H. Lee, S. B. Choi and D.-S. Kim, *Opt. Express*, 2015, 23, 4897-4907.

Physical Chemistry Chemical Physics Accepted Manuscript

28 J. Zuloaga, E. Prodan and P. Nordlander, *Nano Lett.*, 2009, 9, 887-891.

29 R. Esteban, A. G. Borisov, P. Nordlander and J. Aizpurua, *Nat. Commun.*, 2012, 3.

30 S. Nie and S. R. Emory, *Science*, 1997, 275, 1102-1106.

31 K. Kneipp, Y. Wang, H. Kneipp, L. T. Perelman, I. Itzkan, R. Dasari and M. S. Feld, *Phys. Rev. Lett.*, 1997, 78, 1667-1670.

32 K. H. Su, Q. H. Wei, X. Zhang, J. J. Mock, D. R. Smith and S. Schultz, *Nano Lett.*, 2003, 3, 1087-1090.

33 P. K. Jain, W. Y. Huang and M. A. El-Sayed, *Nano Lett.*, 2007, 7, 2080-2088.

34 C. Tabor, R. Murali, M. Mahmoud and M. A. El-Sayed, *J. Phys. Chem. A*, 2009, 113, 1946-1953.

35 B. J. Messinger, K. U. Vonraben, R. K. Chang and P. W. Barber, *Phys. Rev. B*, 1981, 24, 649-657.

36 J. Zuloaga and P. Nordlander, *Nano Lett.*, 2011, 11, 1280-1283.

37 F. Moreno, P. Albella and M. Nieto-Vesperinas, *Langmuir*, 2013, 29, 6715-6721.

38 J. M. Sanz, D. Ortiz, R. Alcaraz de la Osa, J. M. Saiz, F. Gonzalez, A. S. Brown, M. Losurdo, H. O. Everitt and F. Moreno, *J. Phys. Chem. C*, 2013, 117, 19606-19615.

39 B. M. Ross and L. P. Lee, *Opt. Lett.*, 2009, 34, 896-898.

40 P. Alonso-Gonzalez, P. Albella, F. Neubrech, C. Huck, J. Chen, F. Golmar, F. Casanova, L. E. Hueso, A. Pucci, J. Aizpurua and R. Hillenbrand, *Phys. Rev. Lett.*, 2013, 110.

41 C. Menzel, E. Hebestreit, S. Muehlig, C. Rockstuhl, S. Burger, F. Lederer and T. Pertsch, *Opt. Express*, 2014, 22, 9971-9982.

42 D.-S. Kim, J. Heo, S.-H. Ahn, S. W. Han, W. S. Yun and Z. H. Kim, *Nano Lett.*, 2009, 9, 3619-3625.

Physical Chemistry Chemical Physics Accepted Manuscript

43 S. Kessentini, D. Barchiesi, C. D'Andrea, A. Toma, N. Guillot, E. Di Fabrizio, B. Fazio, O. M. Marago, P. G. Gucciardi and M. L. de la Chapelle, *J. Phys. Chem. C*, 2014, 118, 3209-3219.

44 M. Chirumamilla, A. Toma, A. Gopalakrishnan, G. Das, R. P. Zaccaria, R. Krahne, E. Rondanina, M. Leoncini, C. Liberale, F. De Angelis and E. Di Fabrizio, *Adv. Mater.*, 2014, 26, 2353-2358.

45 E. Prodan, C. Radloff, N. J. Halas and P. Nordlander, *Science*, 2003, 302, 419-422.

46 J. Jin, *The Finite Element Method in Electromagnetics*, John Wiley and Sons, New York, 2002.

47 K. L. Wustholz, A. I. Henry, J. M. McMahon, R. G. Freeman, N. Valley, M. E. Piotti, M. J. Natan, G. C. Schatz and R. P. Van Duyne, *J. Am. Chem. Soc.*, 2010, 132, 10903-10910.

48 COMSOL Multiphysics, version 4.4, RF module, http://www.comsol.com.

49 A. D. Rakic, A. B. Djurisic, J. M. Elazar and M. L. Majewski, *Appl. Opt.*, 1998, 37, 5271-5283.

50 E. D. Palik, *Handbook of Optical Constants of Solid*, Academic Press, New York, 1985.

51 C. F. Bohren and D. P. Gilra, *Absorption and Scattering of Light by Small Particles*, Wiley, New York, 1983.

52 V. Giannini, A. I. Fernandez-Dominguez, S. C. Heck and S. A. Maier, *Chem. Rev.*, 2011, 111, 3888-3912.

53 D. L. Jeanmaire and R. P. Van Duyne, *J. Electroanal. Chem.*, 1977, 84, 1-20.

54 K. D. Alexander, K. Skinner, S. Zhang, H. Wei and R. Lopez, *Nano Lett.*, 2010, 10, 4488-4493.

Physical Chemistry Chemical Physics Accepted Manuscript

55 J. Bravo-Abad, L. Martin-Moreno and F. J. Garcia-Vidal, *Phys. Rev. E*, 2004, 69.

56 J. M. McMahon, S. K. Gray and G. C. Schatz, *Phys. Rev. B*, 2011, 83.

57 M. Shanthil, R. Thomas, R. S. Swathi and K. G. Thomas, *J. Phys. Chem. Lett.*, 2012, 3, 1459-1464.

58 J. Chen, P. Albella, Z. Pirzadeh, P. Alonso-Gonzalez, F. Huth, S. Bonetti, V. Bonanni, J. Akerman, J. Nogues, P. Vavassori, A. Dmitriev, J. Aizpurua and R. Hillenbrand, *Small*, 2011, 7, 2341-2347.

59 S. L. Kleinman, B. Sharma, M. G. Blaber, A. I. Henry, N. Valley, R. G. Freeman, M. J. Natan, G. C. Schatz and R. P. Van Duyne, *J. Am. Chem. Soc.*, 2013, 135, 301-308.

Physical Chemistry Chemical Physics Accepted Manuscript

Figure captions

Fig. 1 FEM calculated near-field $\overline{EF}$ (a) and corresponding far-field extinction cross section C_{ext} (b) spectra with 5 nm wavelength spacing for Ag nanosphere (r = 60 nm) dimers. The nanogap size g varies from 1 to 30 nm. The incident polarization is along the interparticle axis. Up tringles symbols in the spectra indicate the bonding dipole mode demonstrated in Fig. 2. See ESI† for detailed spectra of other dimers, including dimers of Ag (r = 30 nm) and Au (r = 30 and 60 nm) nanospheres.

Fig. 2 (Upper row) Local electric field $|E/E_0|^4$ (i.e. near-field EF) distributions at the resonance wavelengths indicated by up triangle symbols in Fig. 1(a). From left to right, the gap size g and resonance wavelengths λ are: (a) g = 1 nm, λ = 700 nm, (b) g = 2 nm, λ = 660 nm, (c) g = 8 nm, λ = 610 nm, and (d) g = 30 nm, λ = 570 nm, respectively. (Bottom row, e-f) Corresponding surface charge distributions of the maximum transient charge polarizations within one oscillation. Red and blue color represent positive and negative charge, respectively. The geometries of single dipole participates into the coupling process are deformed in various degrees. This mapping indicates clearly the bonding dipole mode.

Fig. 3 Log-log plots of $\overline{EF}$ (a) and EF_{max} (b) at the near-field bonding dipole resonance wavelengths as a function of the gap size g for various dimer structures. Fitting parameters A and n for the power-law relationship $\overline{EF}(and\ EF_{\max}) = 10^A \cdot g^n$ are shown in the inserts. The slopes n are about -3.0 and -4.5 for $\log(\overline{EF})$ and $\log(EF_{max})$ against $\log(g)$, respectively.

Physical Chemistry Chemical Physics Accepted Manuscript

Fig. 4 Plots of the extracted near-field and far-field bonding dipole resonance wavelengths λ against the gap size *g* for different Ag (a) and Au (b) dimers. The smooth curves represent least-squares fits to single-exponential decay function $\lambda = \mathrm{a} \cdot e^{-l/g} + \lambda_0$. Fitting parameters *a*, *l* and λ_0 are listed in Table 1. Solid symbols and curves represent the near-field resonance wavelengths and fits, while hollow symbols and dashed curves of the same color represent the corresponding far-field wavelengths and fits for the same dimer structures.

Fig. 5 Calculated near-field $\overline{EF}$ spectra (red curves, corresponding to the right y-axis) and far-field extinction cross section C_{ext} (black curves, corresponding to the left y-axis) with 5 nm wavelength spacing for isolated metallic nanospheres. The near-field and far-field dipole resonance wavelengths are: (a) 390 and 385 nm for *r* = 30 nm Ag nanosphere, (b) 470 and 435 nm for *r* = 60 nm Ag nanosphere, (c) 535 and 495 nm for *r* = 30 nm Au nanosphere, (d) 565 and 530 nm for *r* = 60 nm Au nanosphere, respectively.

Physical Chemistry Chemical Physics Accepted Manuscript

Figures

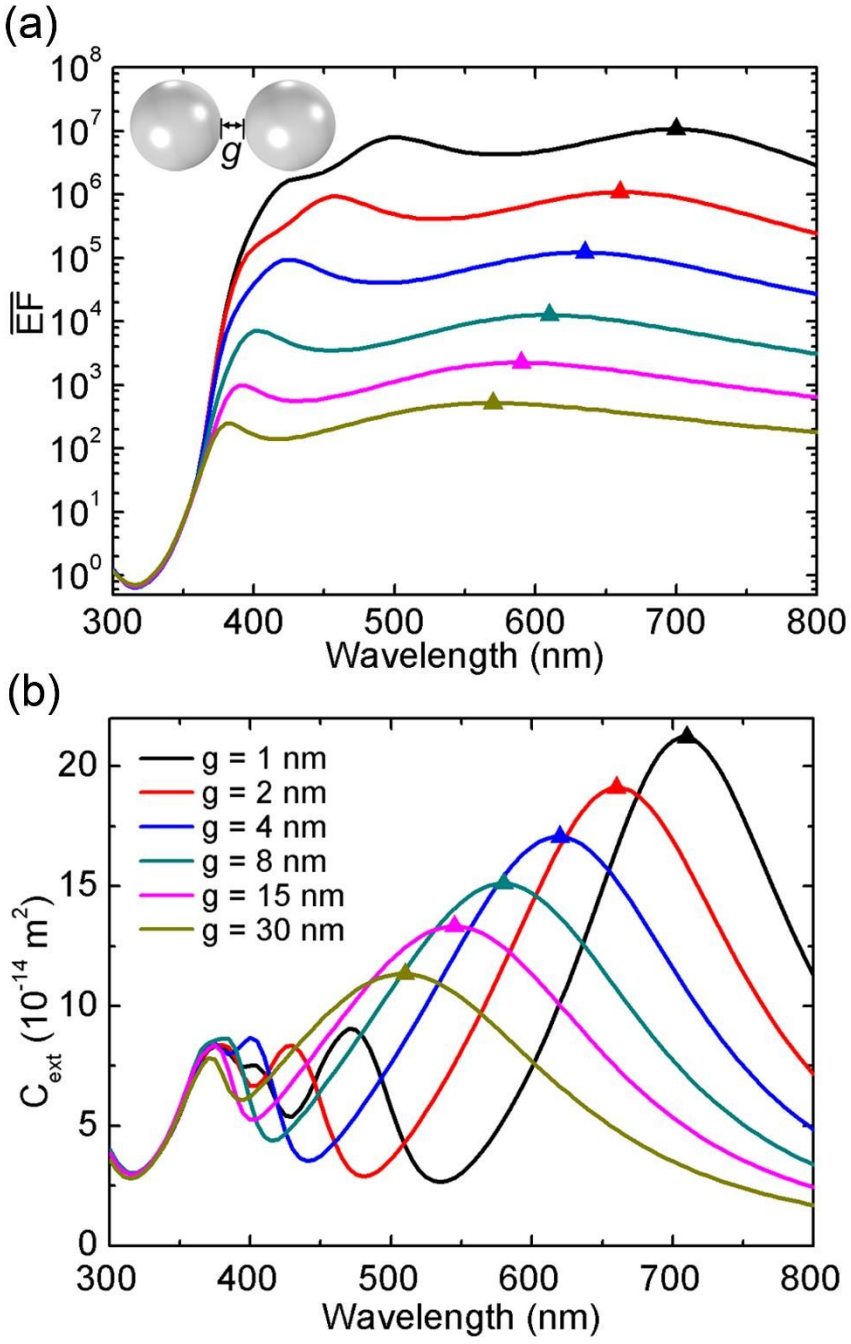

Fig. 1 Huang et al.

Physical Chemistry Chemical Physics Accepted Manuscript

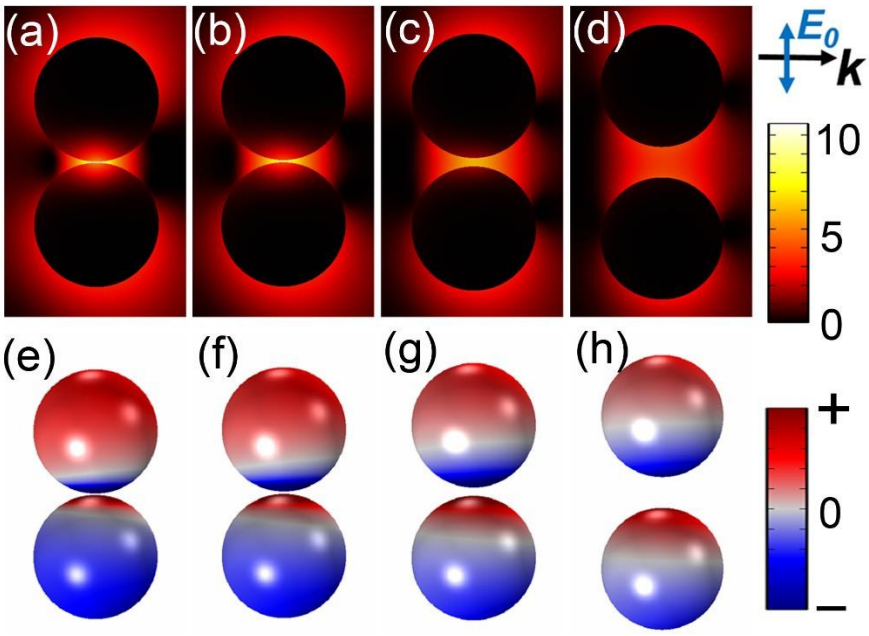

Fig. 2 Huang et al.

Physical Chemistry Chemical Physics Accepted Manuscript

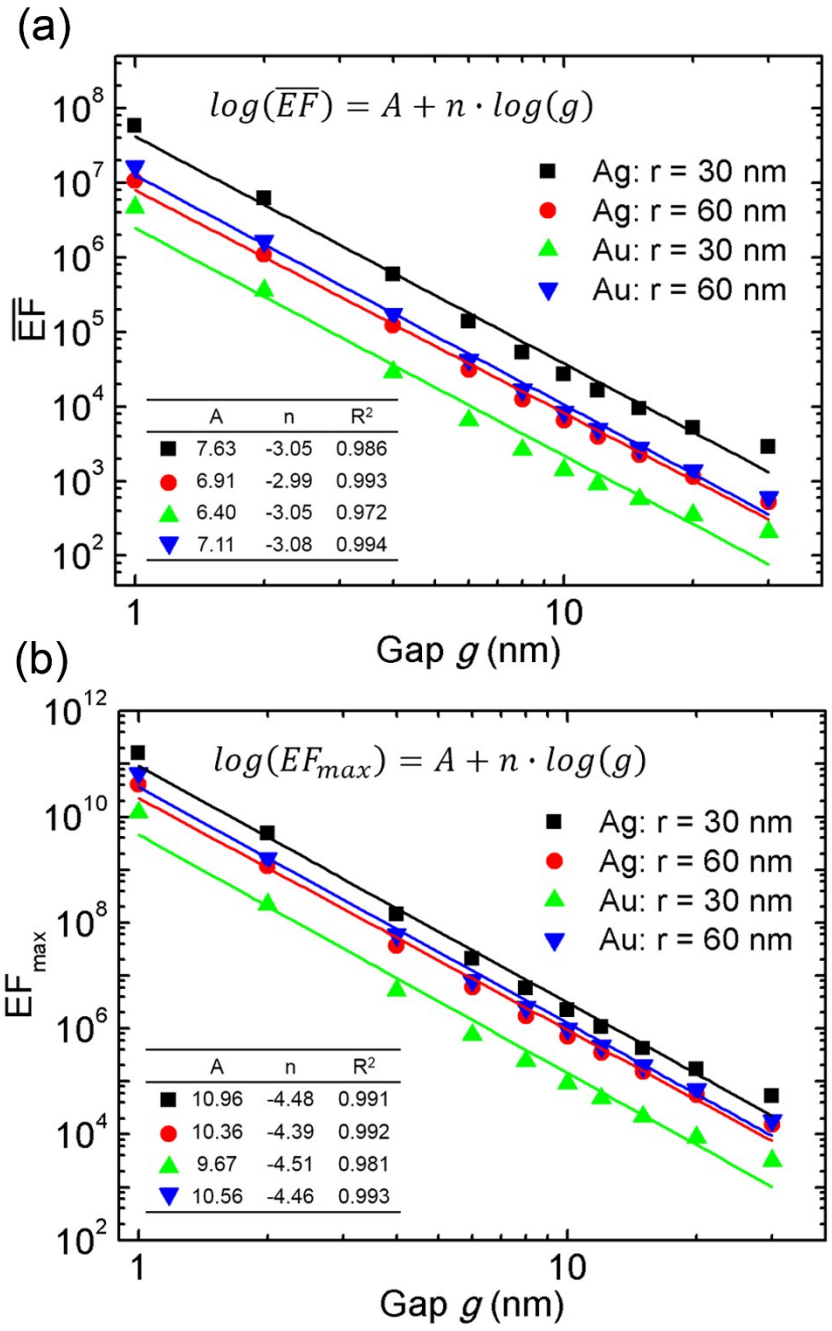

Fig. 3 Huang et al.

Physical Chemistry Chemical Physics Accepted Manuscript

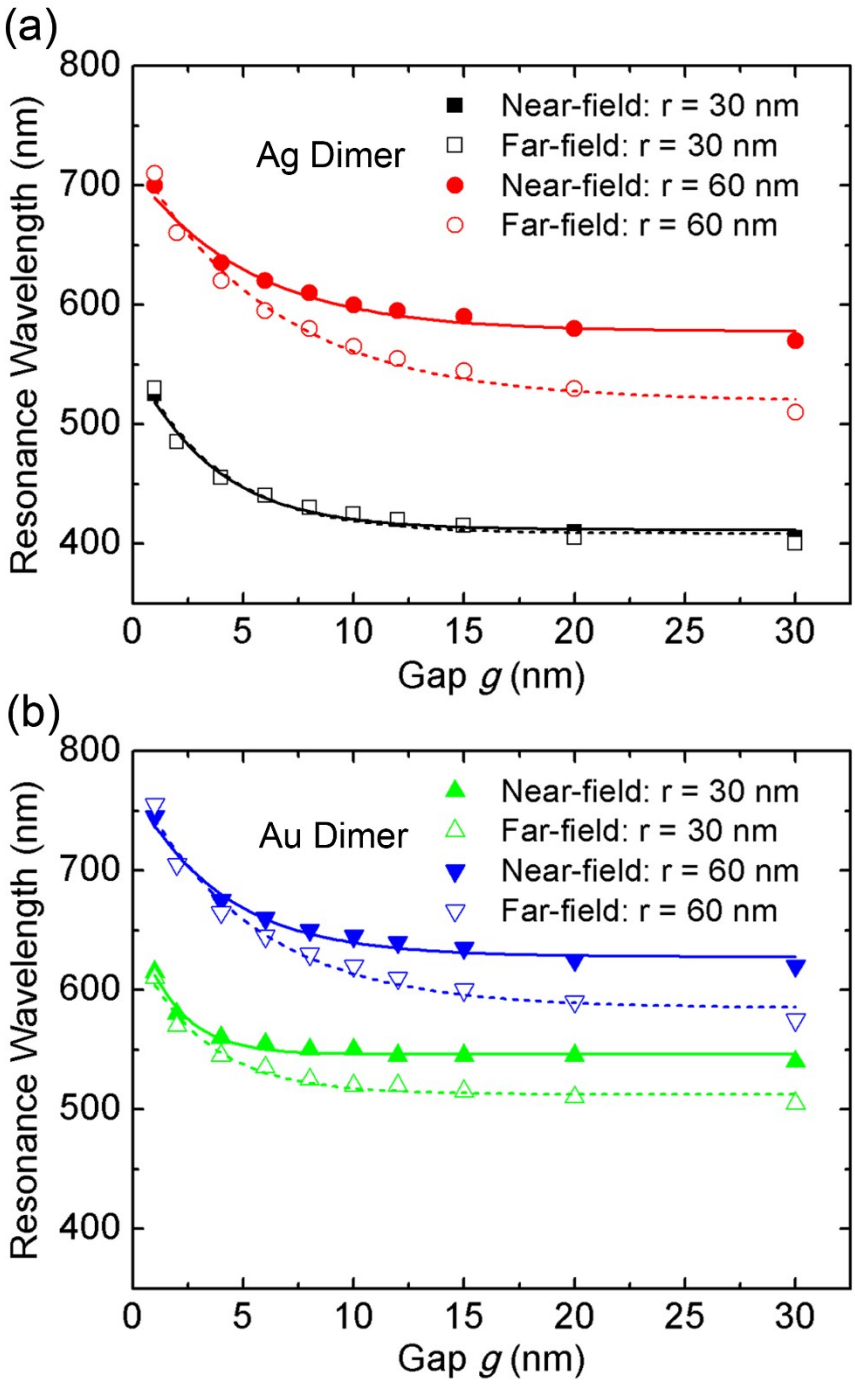

Fig. 4 Huang et al.

Physical Chemistry Chemical Physics Accepted Manuscript

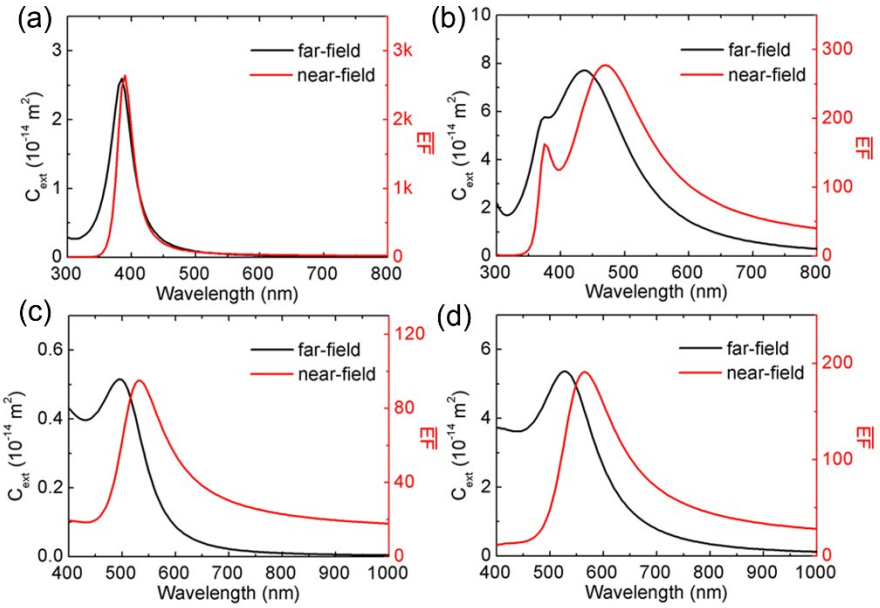

Fig. 5 Huang et al.

Physical Chemistry Chemical Physics Accepted Manuscript

Table 1. List of fitting parameters *a*, *l* and λ_0 for the smooth curves in Fig. 4.

nanosphere dimers	a	l (nm)	λ_0 (nm)	R^2
Ag: r = 30 nm (near-field)	141.7	3.61	411.5	0.980
Ag: r = 30 nm (far-field)	147.3	3.78	408.6	0.966
Ag: r = 60 nm (near-field)	136.6	5.20	577.4	0.968
Ag: r = 60 nm (far-field)	208.9	6.23	519.2	0.977
Au: r = 30 nm (near-field)	115.7	1.82	546.0	0.971
Au: r = 30 nm (far-field)	126.4	3.10	512.6	0.967
Au: r = 60 nm (near-field)	140.6	4.05	627.7	0.971
Au: r = 60 nm (far-field)	191.5	5.27	584.8	0.974

Physical Chemistry Chemical Physics Accepted Manuscript

Electronic Supplementary Information (ESI) for

Nanogap Effects on Near- and Far-Field Plasmonic Behaviors of Metallic Nanoparticle Dimers

Yu Huang,[a] Qin Zhou,[b] Mengjing Hou,[a] Lingwei Ma[a] and Zhengjun Zhang*[c]

[a] *State Key Laboratory of New Ceramics and Fine Processing, School of Materials Science and Engineering, Tsinghua University, Beijing 100084, P. R. China*

[b] *Institute of Nuclear and New Energy Technolog, Tsinghua University, Beijing 100084, P. R. China*

[c] *Key Laboratory of Advanced Materials (MOE), School of Materials Science and Engineering, Tsinghua University, Beijing 100084, P. R. China. E-mail: zjzhang@tsinghua.edu.cn*

Physical Chemistry Chemical Physics Accepted Manuscript

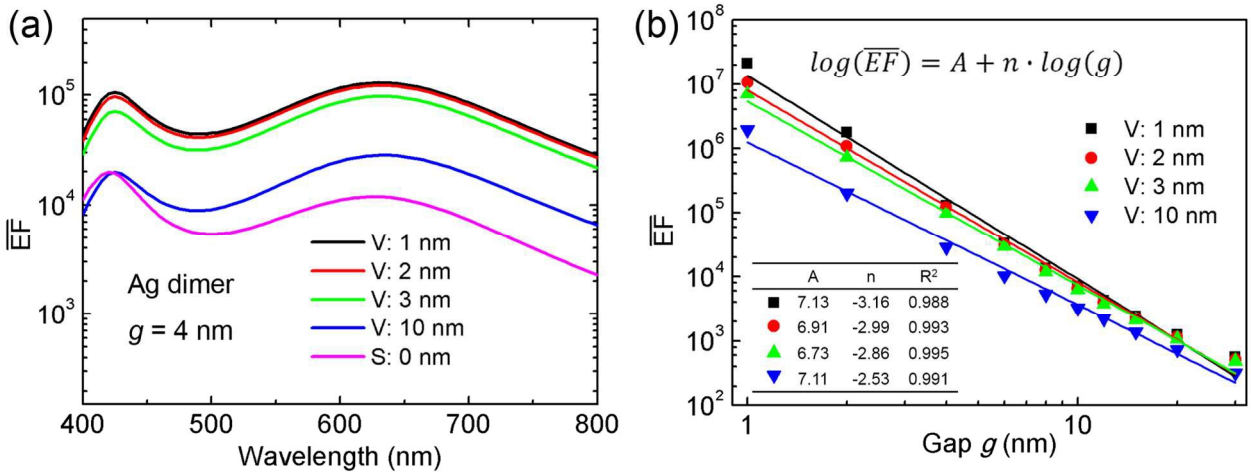

Fig. S1. (a) Calculated $\overline{EF}$ spectra for Ag nanosphere dimer (r = 60 nm, g = 4 nm, as an example) with different expressions of $\overline{EF}$ which are the average of the volume integral of $|\boldsymbol{E}|^4/|\boldsymbol{E}_{inc}|^4$ within 1 nm (black curve), 2 nm (red curve), 3 nm (green curve) and 10 nm (blue curve) above the metal surface, and the surface integral of $|\boldsymbol{E}|^4/|\boldsymbol{E}_{inc}|^4$ at the metal surface (magenta curve). Note that the curve shape and peak positions for different volume integral do not change while both exhibit changes for the surface integral. (b) Log-log plots of $\overline{EF}$ acquired from different volume integral as a function of the gap size g for dimers of Ag nanospheres (r = 60 nm). Fitting parameters A and n for the nearly power-law relationship $\overline{EF} = 10^A \cdot g^n$ are shown in the insert. The value of n increases from -3.16 to -2.53 as the distance above the metal surface for the volume integral increases from 1 to 10 nm.

Physical Chemistry Chemical Physics Accepted Manuscript

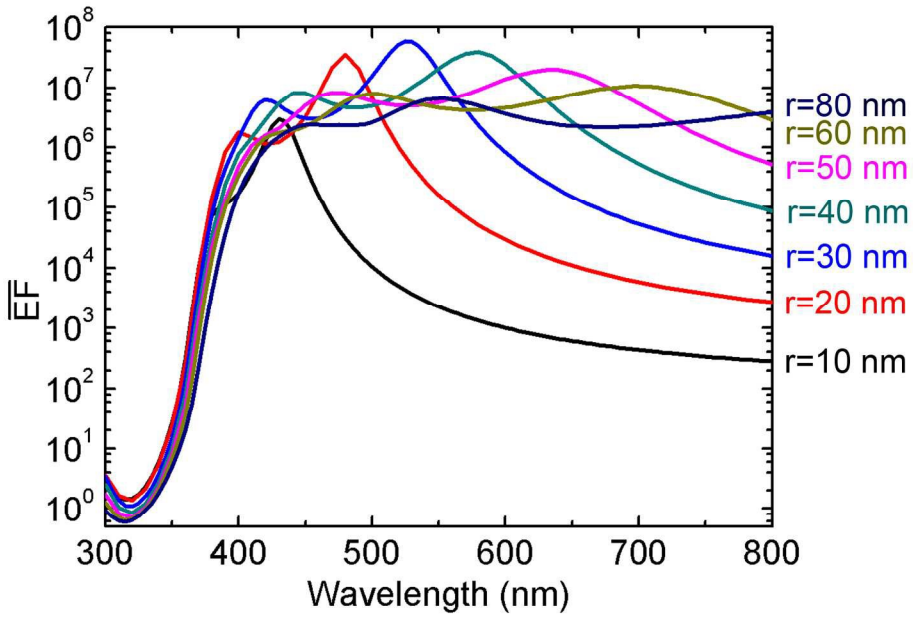

Fig. S2. Calculated near field $\overline{EF}$ spectra by fixing the gap size g = 1 nm and varying Ag nanosphere radius *r* from 10 to 80 nm. The near field enhancement becomes almost 'flat' in the visible range when *r* > 50 nm. As is known, for large individual plasmonic nanospheres (e.g. *r* > 50 nm), multipole resonances can be excited besides the fundamental dipole resonance. For the dimer structure, the continuous arising of bonding dipole resonances in longer wavelength regions and bonding multipole resonances in shorter wavelength regions can lead to the flat near field enhancement.

Physical Chemistry Chemical Physics Accepted Manuscript

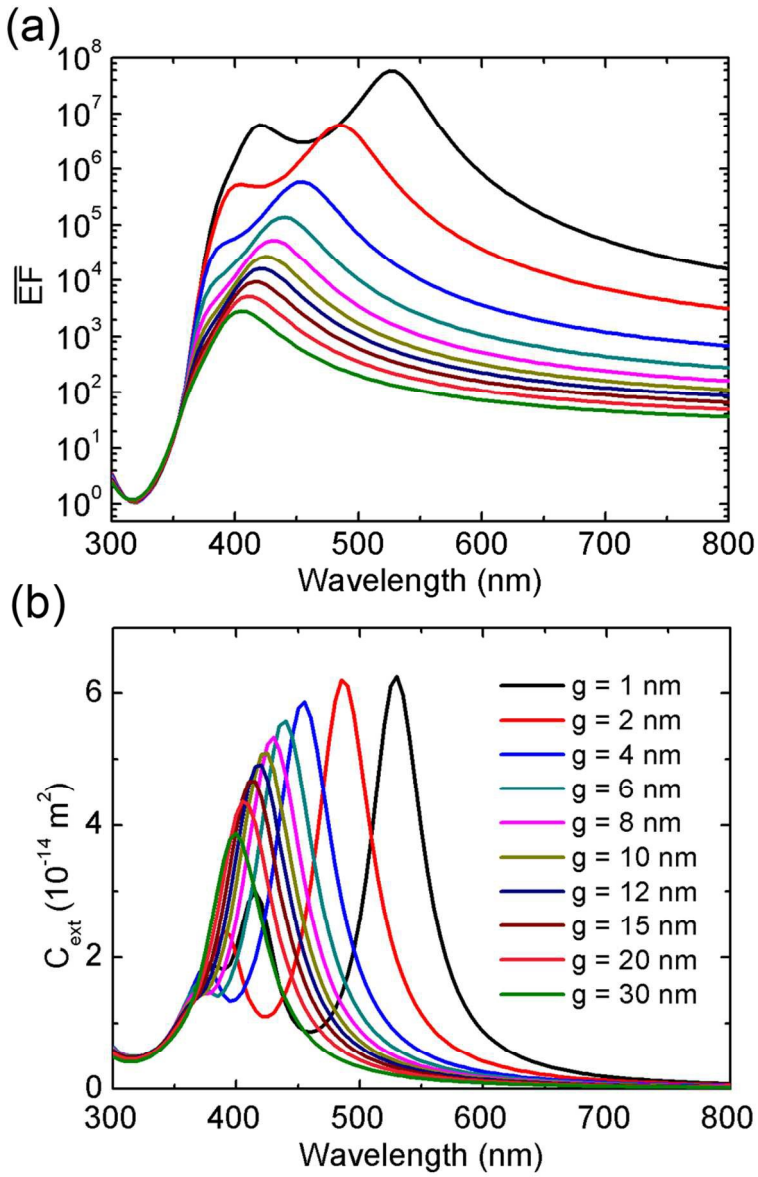

Fig. S3. FEM calculated near-field $\overline{EF}$ (a) and corresponding far-field extinction cross section C_{ext} (b) spectra with 5 nm wavelength spacing for Ag nanosphere (r = 30 nm) dimers. The gap size g varies from 1 to 30 nm.

Physical Chemistry Chemical Physics Accepted Manuscript

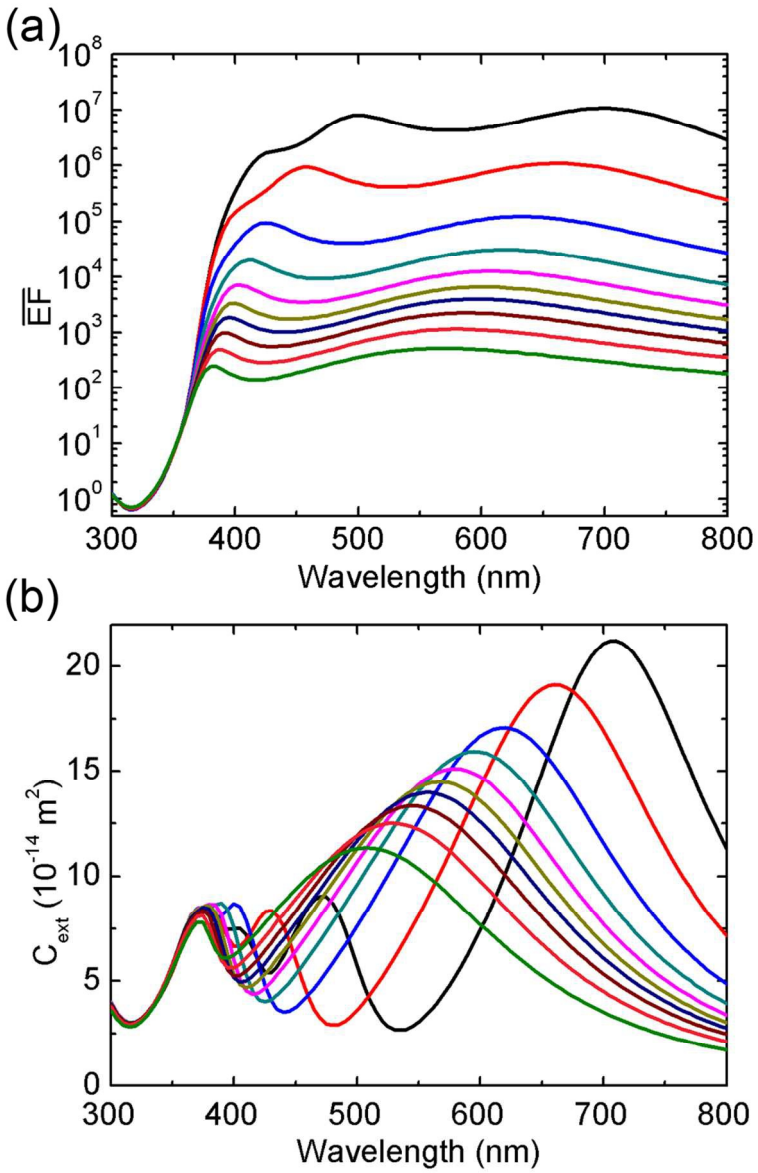

Fig. S4. $\overline{EF}$ and corresponding C_{ext} spectra with 5 nm wavelength spacing for Ag nanosphere (r = 60 nm) using the same legend as in Fig. S2.

Physical Chemistry Chemical Physics Accepted Manuscript

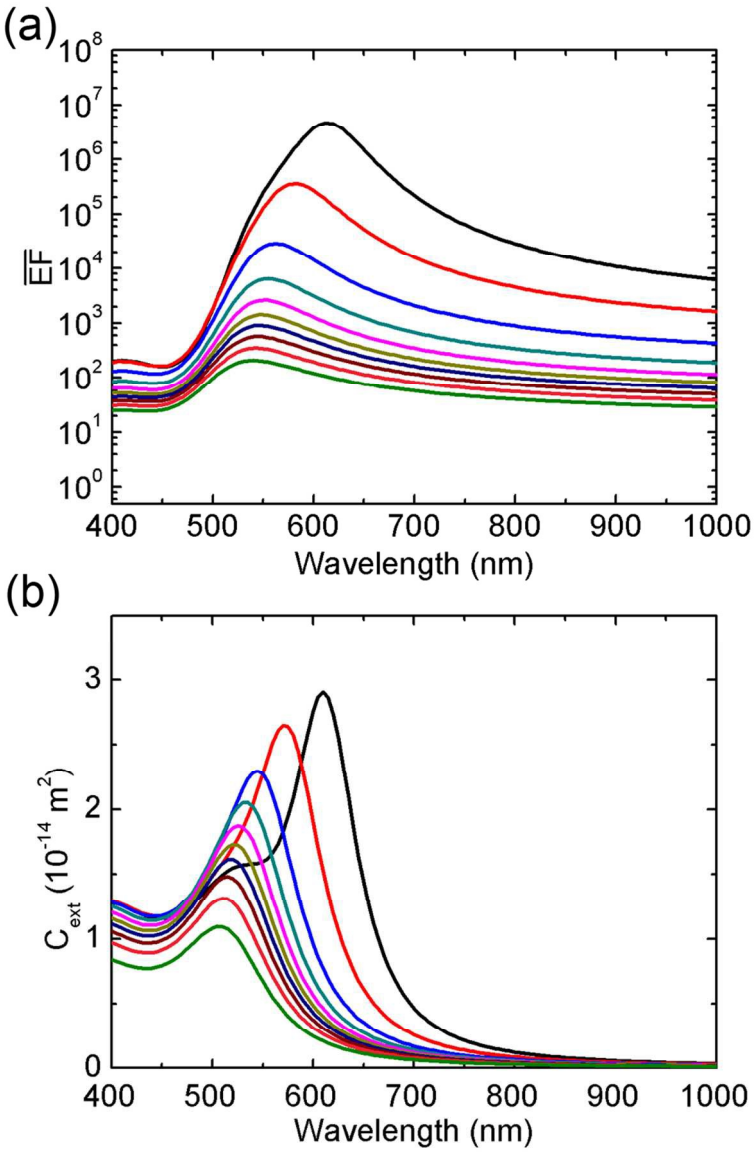

Fig. S5. $\overline{EF}$ and corresponding C_{ext} spectra with 5 nm wavelength spacing for Au nanosphere (r = 30 nm) using the same legend as in Fig. S2.

Physical Chemistry Chemical Physics Accepted Manuscript

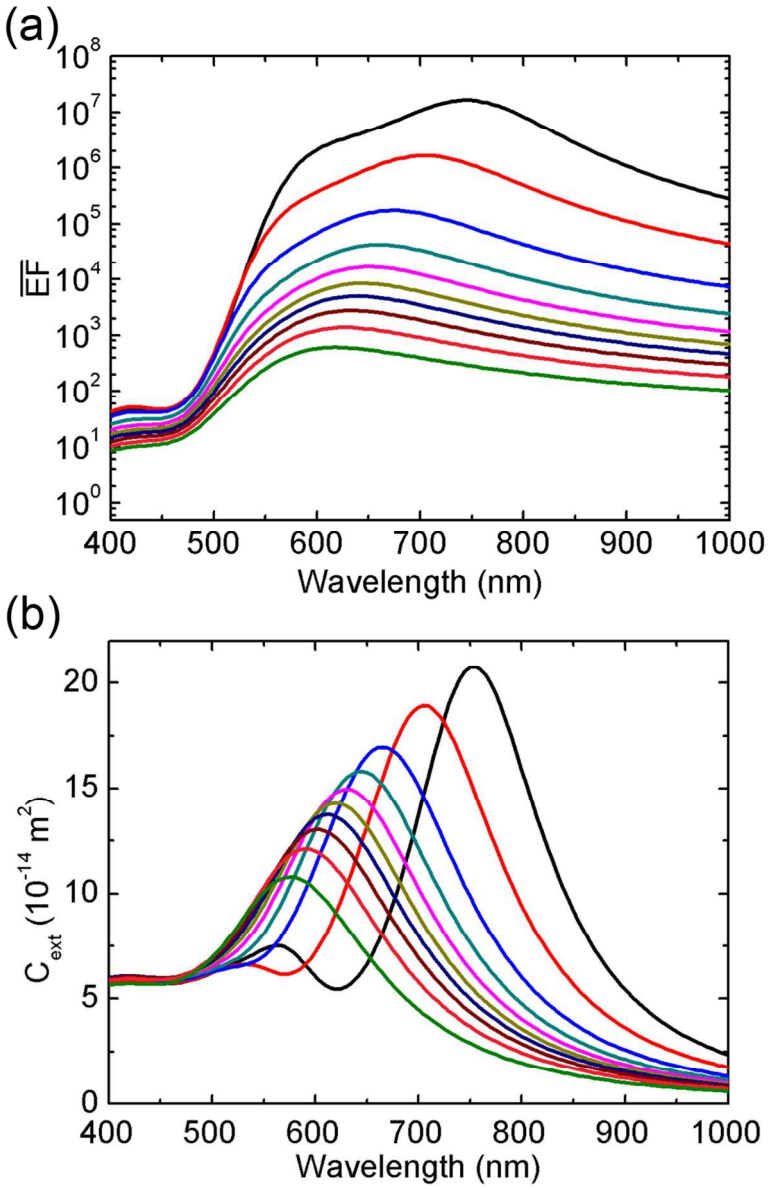

Fig. S6. $\overline{EF}$ and corresponding C_{ext} spectra with 5 nm wavelength spacing for Au nanosphere (r = 60 nm) using the same legend as in Fig. S2.

Physical Chemistry Chemical Physics Accepted Manuscript

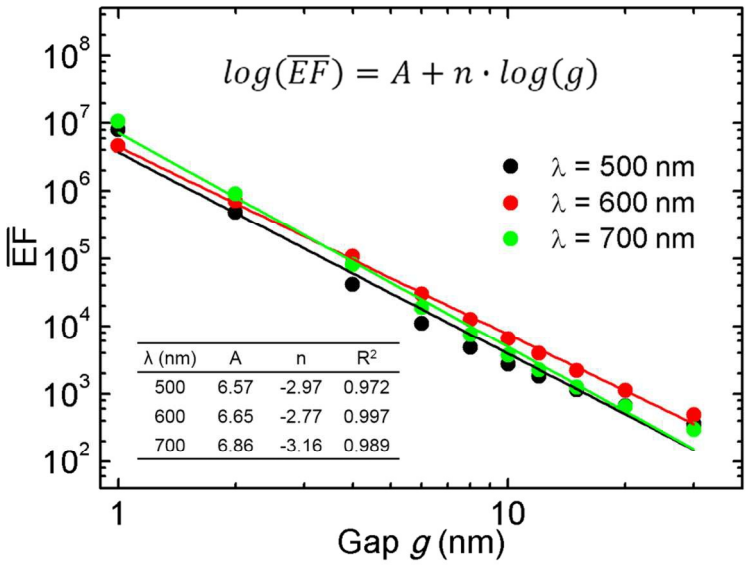

Fig. S7. Log-log plots of $\overline{EF}$ values at λ = 500, 600 and 700 nm as a function of the gap size g for r = 60 nm Ag nanosphere dimer. The slopes n are -2.97, -2.77 and -3.16 respectively.

Movie S1: Three dimensional surface charge distributions within one full oscillation for Fig. 2(e).

Physical Chemistry Chemical Physics Accepted Manuscript